

Star cluster systems in nearby spiral galaxies. Case: Globular clusters



Mc. Luis Fernando Lomelí Núñez
Dr. Yalia Divakara Mayya
Dr. Lino Hector Rodríguez Merino
Mc. Pedro Antonio Ovando
8 de junio de 2021

Generalities:

- What are we going to study?
We will study the stellar populations the **stellar populations** in a sample of **nearby spiral galaxies**: M81 (Santiago-Cortéz et al. 2010), M101 (Simanton et al. 2015), NGC 4258, M51 (Hwang et al. 2008) y NGC 628 (NGC 1300, NGC 1483, NGC 2397 NGC 1309).
- How are we going to do it?
Performing a **photometric** and **spectroscopy** analysis.
- Photometric data: we use images observed with Advance Camera for Surveys on board Hubble Space Telescope (**ACS/HST**) F435W (B), F555W (V) y F814W (I) bands and F336W (U) (**WFC3/HST**).
- Spectroscopic data: we used **OSIRIS/GTC** data, taked with R1000B grism (3650-10000 Å). Time obtained with the Mexican participation time.
- **Probably** spectroscopic data from **MEGARA/GTC**.

Goals:

- 1.- In this work the principal objective is establish the presence of **Super Stellar Compact (SSC)**, in a sample of spiral galaxies nearby. These SSCs are believed to be the 'link' between a middle-aged cluster and a globular cluster (GC). **(In this presentation only I establish the presence of SSC).**
- 2.- Study the evolution of **Luminosity Function (LF)** of SSC at different ages. **(Here the globular cluster LF is only present).**
- 3.- Estimate the **Stellar Formation History (SFH)**, through SSC of different ages.
- 4.- Determine the importance of **interactions** in the formation and evolution of galaxies.

Stellar clusters (a brief introduction):

Open clusters*:

- Type I.
- Young ($<10^6$ años).
- Blue.
- Metal-rich.
- Disk and core.

Globular clusters**:

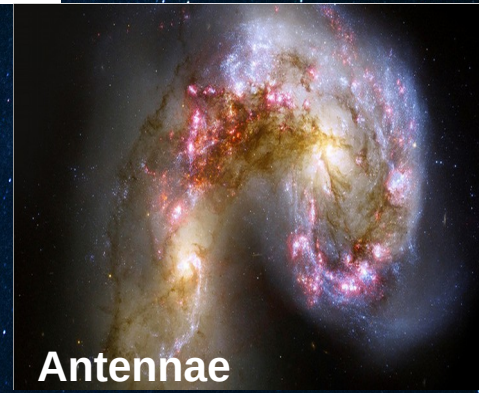
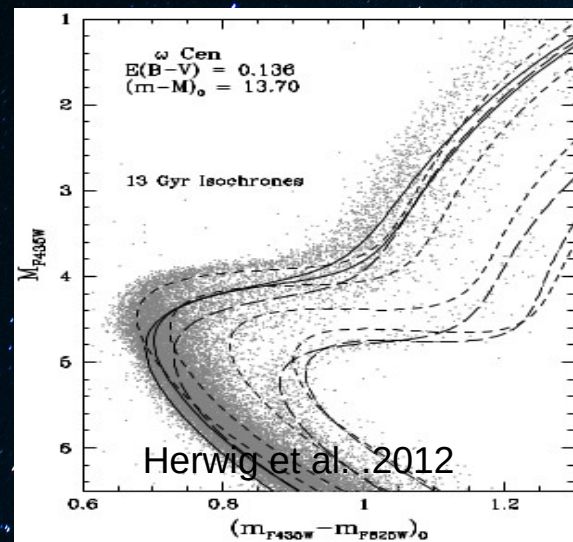
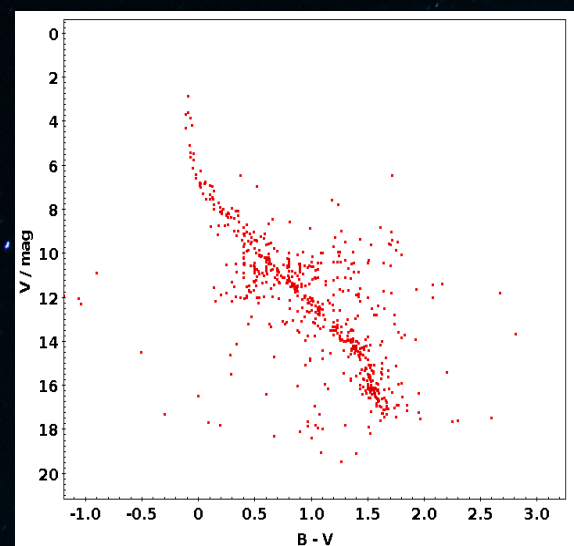
- Type II.
- Old (10^9 años).
- Red.
- Metal-poor.
- Halo

Compact clusters***:

- Starburst galaxies
- Sizes ($r_e < 10$ pc) and masses ($10^5 M_{\text{sun}}$)
- Super Stellar cluster (SSC) are the most massive.
- Ages between: open and GC. Transition clusters?

Faint Fuzzy clusters****:

- Extended ($7 < r_e < 15$ pc).
- Faint ($M_v = -6$ to -7).
- Colours like a GCs.



* eg., Ryon, et al. (2015)
 **eg., Brodie & Strader (2006)
 ***eg., Whitmore et al. (1999)
 ****eg., Larsen & Brodie (2000)

Sample of galaxies:



- Nearby spiral galaxies (~4-30 Mpc). In this talk I present the results for galaxies within 10 Mpc.
- Spatial observational coerture in two HST filters: F435W and F814W, F555W (0.05 arcsec/pix) and F336W (0.04 arcsec/pix).
- Galaxies with super stellar clusters.

Name	Hubble Type	RA (J2000)	DEC (J2000)	A_V (mag)	R_{25} (')	a_{\max} (')	d (Mpc)	$m - M$ (mag)	Distance method	Source	M_{V_0}	$(B - V)_0$	Scale (pc)	Source SSCs	Proposal ID	Number of fields
(1)	(2)	(3)	(4)	(5)	(6)	(7)	(8)	(9)	(10)	(11)	(12)	(13)	(14)	(15)	(16)	(17)
M81	Sab	09:55:33.1	69:03:55	0.220	13.45	7.74	3.61	27.79±0.06	Cepheids	1	-21.10	0.91	0.87	1,2	11570	29
NGC1313	SBd	03:18:16.05	-66:29:53	0.362	4.56	3.73	4.60	28.32±0.08	Cepheids	2	-19.97	0.38	1.11	3	9774	3
M101	Scd	14:03:12.5	54:20:56	0.023	14.42	7.49	6.95	29.21±0.06	Cepheids	3	-21.37	0.44	1.68	5,7,8	9490,9492	12
NGC4258	Sbc	12:18:57.5	47:18:14	0.045	9.31	8.60	7.576	29.397±0.032	MASER	4	-21.03	0.67	1.84	4	1157	17
M51	Sbc	13:29:56.2	47:13:50	0.095	5.61	3.40	8.43	29.67±0.02	SNII	5	-21.40	0.57	2.04	5,6	10452	6(4)
NGC628	Sc	01:36:41.7	15:47:01	0.192	5.23	5.1	9.77	29.95±0.04	SNII	6	-20.75	0.50	2.36	5,9	10402	3
NGC1300	SBbc	03:19:41.0	-19:24:40	0.083	3.08	3.08	14.50	30.81±0.40	Tully-Fisher	7	-20.46	0.63	3.51	5	10342	2
NGC1483	SBbc	03:52:47.6	-47:28:39	0.019	0.81	0.81	18.70	31.36±0.47	Tully-Fisher	8	-18.70	0.42	4.53	5	9395	1
NGC2397	SBb	07:21:20.0	-69:00:05	0.562	1.22	1.22	19.80	31.48±0.45	Tully-Fisher	9	-20.21	0.67	4.79	5	10498	1
NGC1309	SABc	03:22:06.5	-15:24:00	0.110	1.09	1.09	30.20	32.40±0.06	Cepheids	10	-20.98	0.37	7.32	5	10497	1

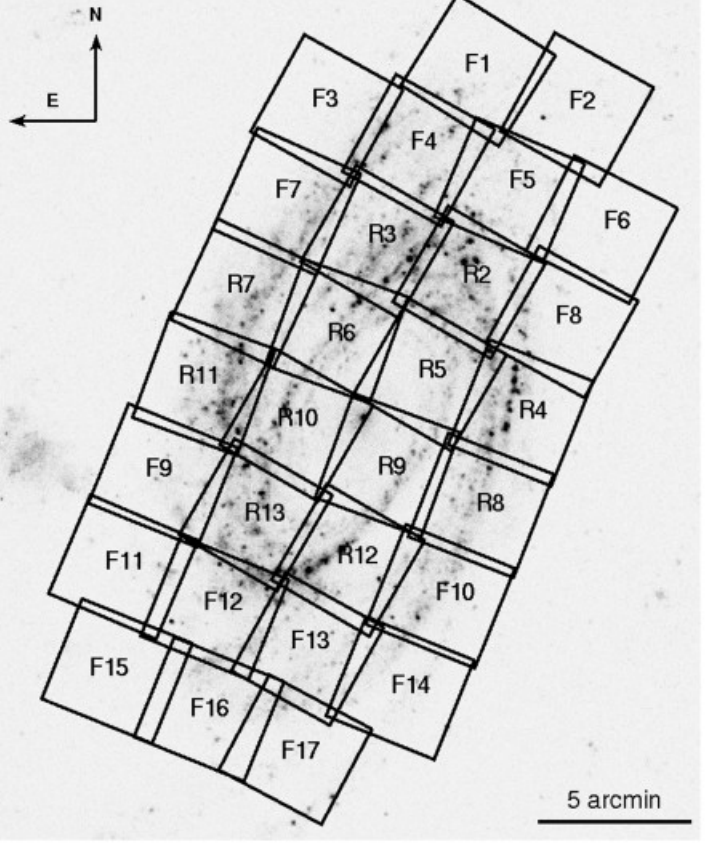
Notes: (1) Galaxy Name, (2) Hubble morphological type from RC3 (Corwin et al. 1994), (3,4) Right ascension, Declination, in J2000, (5): Galactic extinction from Schlafly & Finkbeiner (2011), (6) R_{25} from RC3 (Corwin et al. 1994), (7) a_{\max} is the semi-major axis covered by observations, (8) Distance used in this work, (9) Distance modulus, (10) Distance estimation method, (11) Source of distances: 1.- Tully et al. (2013); 2.- Qing et al. (2015); 3.- Riess et al. (2016), 4.- Reid et al. (2019); 5.- Rodríguez et al. (2014); 6.- Olivares E. et al. (2010), (12,13) Absolute magnitude in V band and $(B - V)_0$ colour from RC3 (Corwin et al. 1994), (14) HST/ACS pixel scale in pc pixel⁻¹, (15) References to previous studies of stellar clusters: 1.- Santiago-Cortés et al. (2010); 2.- Nantais et al. (2010); 3.- Ryon et al. (2017); 4.- González-Lópezlira et al. (2017); 5.- Whitmore et al. (2014); 6.- Hwang & Lee (2008); 7 Barmby et al. (2006); 8 Simanton et al. (2015b); 9 Adamo et al. (2017), (16) HST proposal number, (17) Number of ACS fields of each galaxy used in this work.

Sample of galaxies:

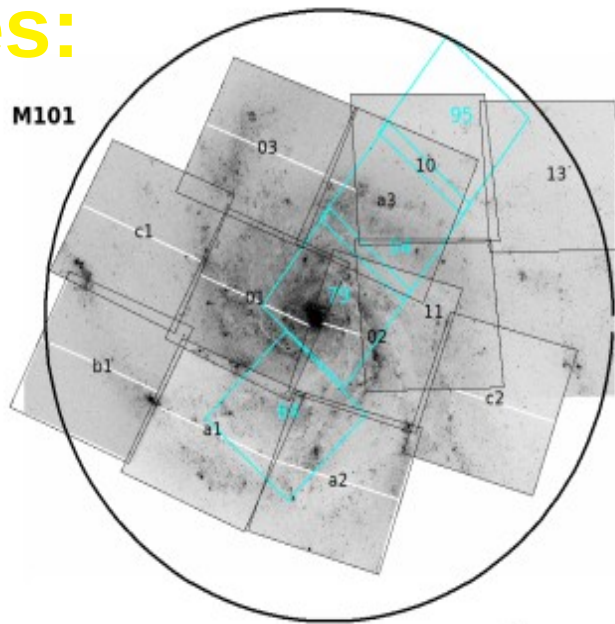
M81

SDSS9 color

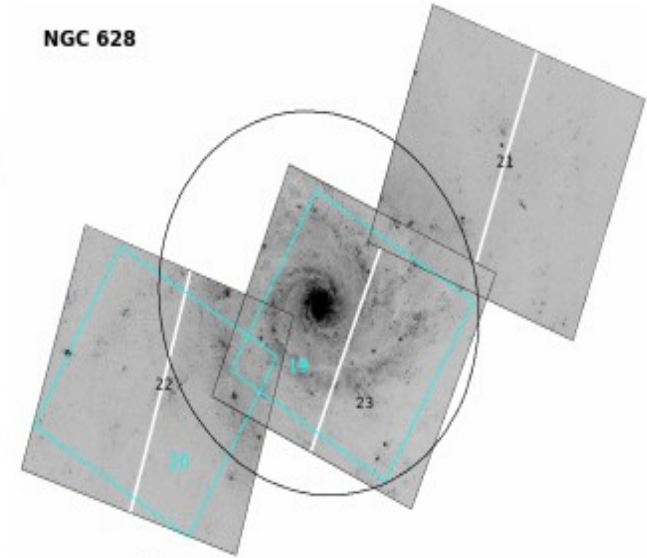
SDSS9



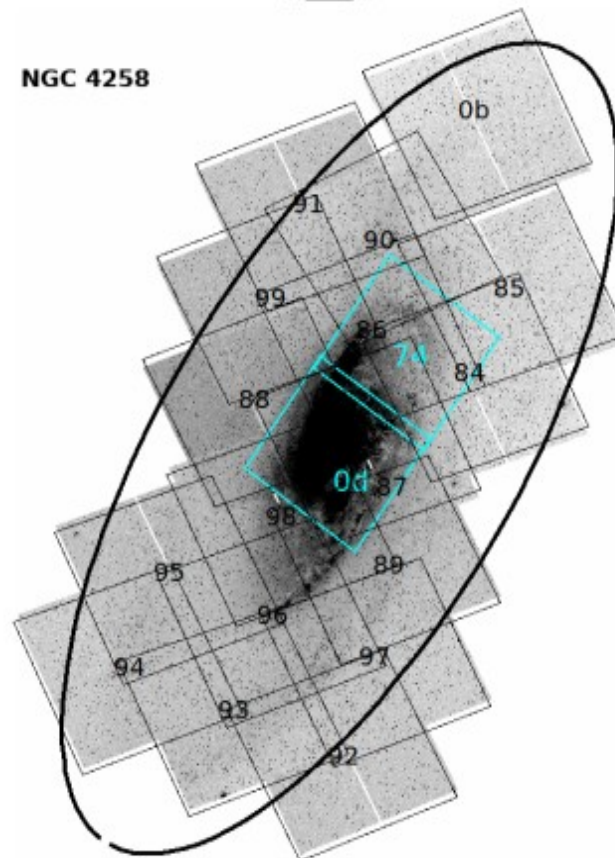
M101



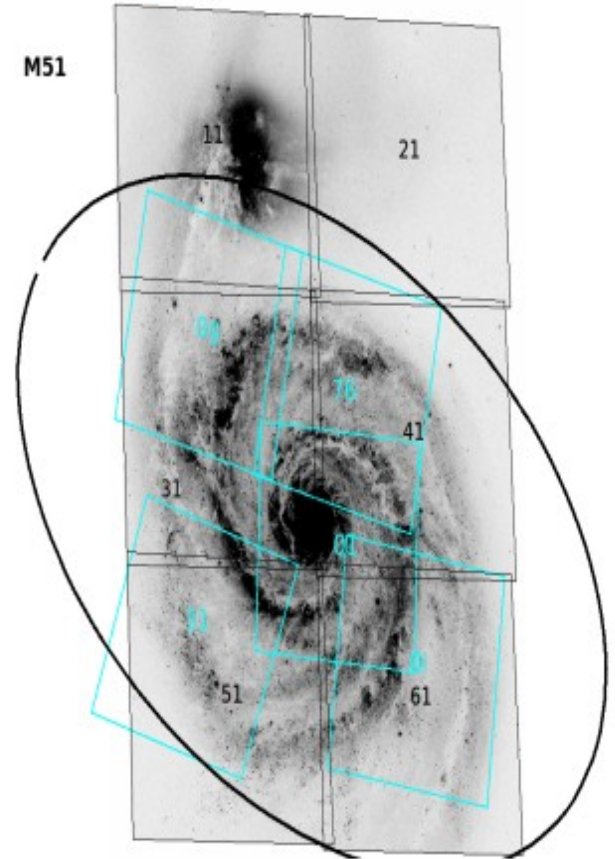
NGC 628



NGC 4258



M51



8 de junio 2021

Astrometry, detection and photometry:

Astrometry: we correct the angular coordinates using GAIA and ccmmap IRAF task with a second order polynomial in coordinates.

Detection and photometry: We employ the SExtractor software (v2.19.5), for detection (Table 2) and photometry (Table 1). We made photometry aperture.

Galaxy (1)	All N_{SSC+GC} (2)	NGC (3)	N_{GC}^U/N_{GC} (4)	N_{cont}/N_{GC} (5)	(6)
M81	565438	433	158	0.65	0.20
M101	1215533	3503	1202	0.15	0.31
NGC4258	1360607	936	334	0.38	0.33
M51	452747	1196	293	0.52	0.25
NGC628	224108	608	173	0.41	0.14

Table 3.- Source detection and stellar cluster selection.

8 de junio 2021

Table 2.- Log of HST/ACS optical observations of our sample galaxies.

ID	F435W		F555W		F814W		Astrometric	
	T_{exp} (s)	c0	T_{exp} (s)	c0	T_{exp} (s)	c0	N_{stars}	RMS (arcsec)
M101								
01	900	25.792	720	25.736	720	25.531	93	0.0259
02	900	25.792	720	25.736	720	25.531	55	0.163
03	900	25.792	720	25.736	720	25.531	38	0.0385
a1	900	25.792	720	25.736	720	25.531	41	0.0319
a2	900	25.792	720	25.736	720	25.531	37	0.278
a3	900	25.792	720	25.736	720	25.531	11	0.0766
b1	900	25.792	720	25.736	720	25.531	10	0.187
c1	900	25.792	720	25.736	720	25.531	18	0.0925
c2	900	25.792	720	25.736	720	25.531	21	0.0175
10	1080	25.792	1080	25.736	1080	25.531	13	0.0988
11	1080	25.792	1080	25.736	1080	25.531	29	0.0456
13	1080	25.792	1080	25.736	1080	25.531	11	0.0862
NGC 4258								
0b	360	25.767	975	25.717	375	25.520	6	0.0134
84	360	25.767	975	25.717	375	25.520	8	0.0264
85	360	25.767	975	25.717	375	25.520	6	0.0058
86	360	25.767	975	25.717	375	25.520	27	0.0049
87	360	25.767	975	25.717	375	25.520	35	0.0049
88	360	25.767	975	25.717	375	25.520	26	0.0051
89	360	25.768	975	25.717	375	25.521	12	0.0023
90	360	25.767	975	25.717	375	25.520	13	0.0090
91	360	25.767	975	25.717	375	25.520	5	0.039
92	360	25.768	975	25.717	375	25.521	8	0.025
93	360	25.768	975	25.717	375	25.521	9	0.0273
94	360	25.768	975	25.717	375	25.521	9	0.03
95	360	25.768	975	25.717	375	25.521	8	0.0145
96	360	25.768	975	25.717	375	25.521	20	0.0157
97	360	25.768	975	25.717	375	25.521	8	0.0054
98	360	25.768	975	25.717	375	25.521	30	0.0054
99	360	25.767	975	25.717	375	25.520	14	0.0128
M51								
1-6	680×4	25.888	340×4	25.715	340×4	25.471	299	0.0482
NGC 628								
21	1200	25.789	1000	25.732	900	25.528	9	0.0445
22	800	25.788	360	25.731	720	25.528	15	0.047
23	1358	25.789	858	25.732	922	25.528	15	0.034

Table 2.- Log of HST/WFC3 F336W-band observations of our sample galaxies.

ID (1)	T_{exp} (s) (2)	c0 (3)	N_{stars} (4)	RMS (arcsec) (5)	Proposal ID (6)
M101					
64	2361	23.546	-	-	13364
79	2382	23.546	-	-	13364
94	2382	23.546	-	-	13364
95	2382	23.546	-	-	13364
NGC 4258					
0d	1062	23.546	33	0.0154	13364
74	1062	23.546	15	0.0109	13364
M51					
01	4360	23.546	163	0.0352	13340
0g	2376	23.546	55	0.0191	13364
0i	2361	23.546	42	0.0317	13364
76	2376	23.546	64	0.0281	13364
31	780	23.546	31	0.0350	14149
NGC 628					
19	2361	23.546	15	0.0031	13364
20	1119	23.546	10	0.0321	13364

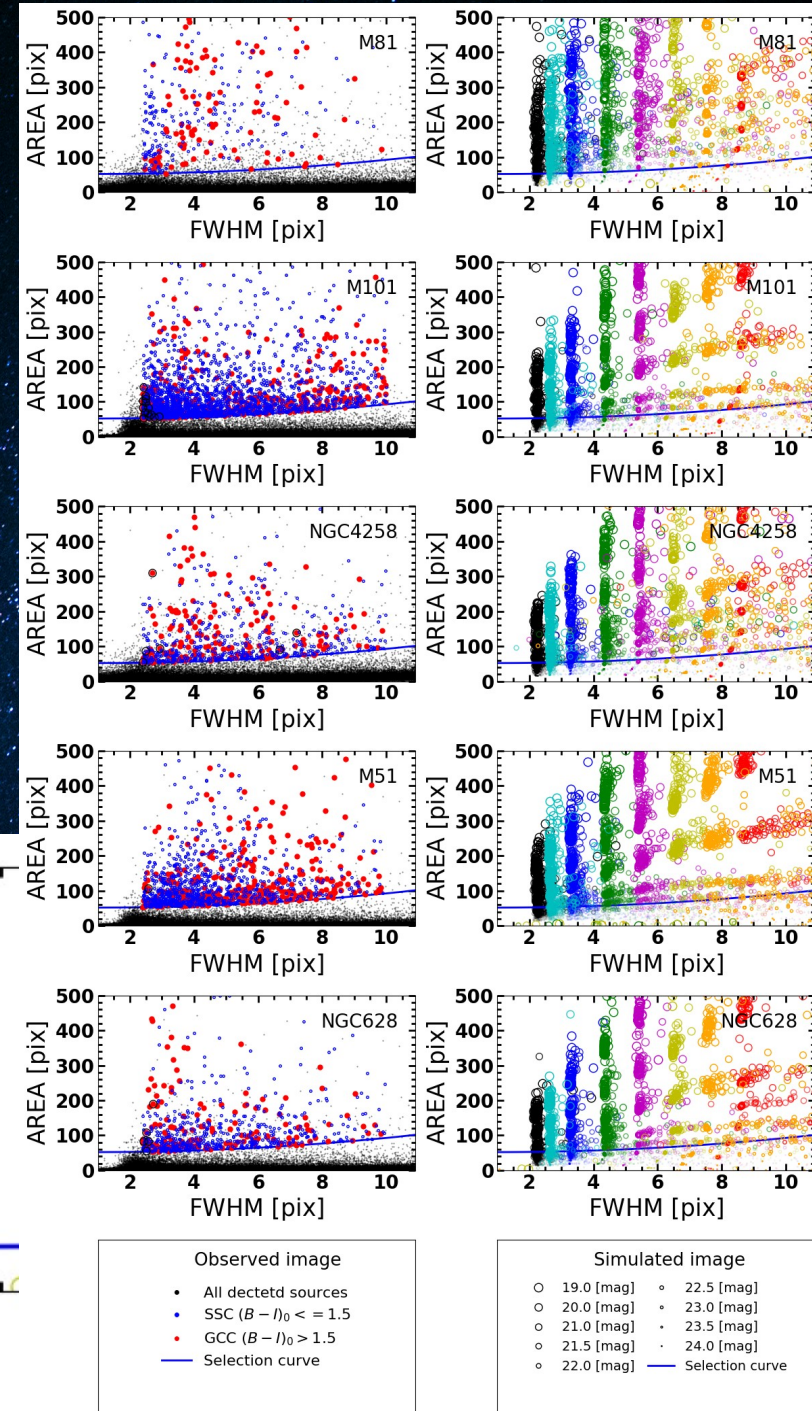
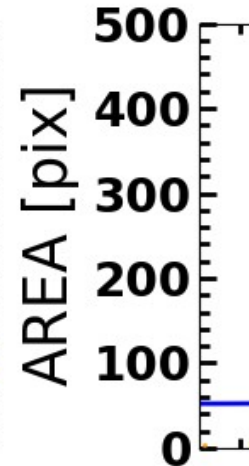
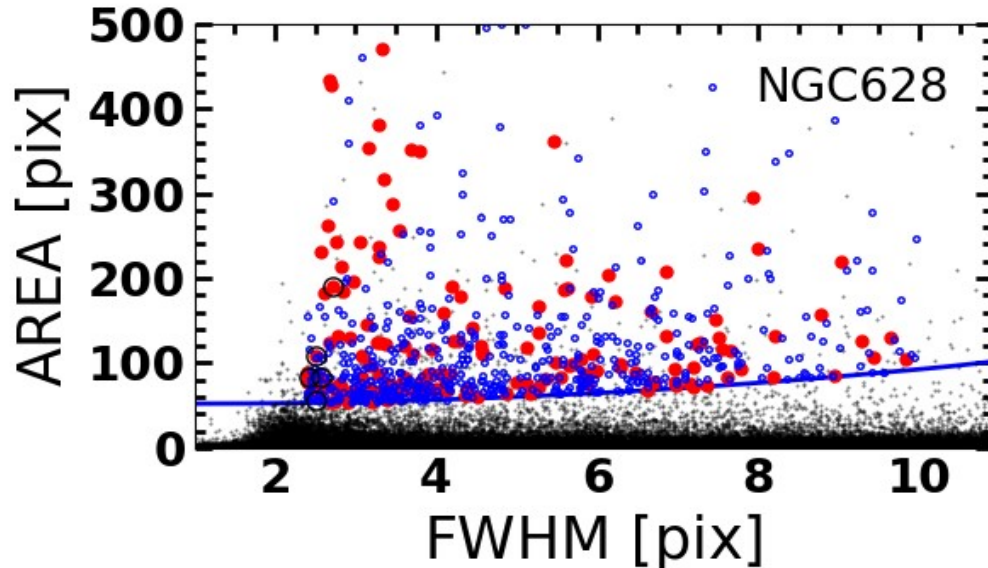
Field ID	Filter	Proposal ID	Exp. time (s)
F1	F435W	10584	1 × 900
F1	F606W	10584	1 × 880
F1	F814W	10584	1 × 895
F2	F435W	10584	3 × 1565
F2	F606W	10584	3 × 1580
F2	F814W	10584	3 × 1595
F3-F14	F435W	10584	2 × 1200
F3-F14	F606W	10584	2 × 1200
F3-F10	F814W	10250	3 × 1650
F11	F814W	10250	2 × 1100
F12-F14	F814W	10250	3 × 1650
F15-F16	F435W	10584	3 × 1565
F15-F16	F606W	10584	3 × 1580
F15-F16	F814W	10584	3 × 1595
F17	F435W	10584	2 × 665
F17	F606W	10584	1 × 350
F17	F814W	10584	1 × 350
R2-R13	F435W	10584	2 × 1200
R2-R13	F606W	10584	2 × 1200
R2-R13	F814W	10250	3 × 1650

Selection of Super Stellar Clusters:

Structural parameters: a SSC must satisfy with: $2.4 < \text{FWHM} < 10$, $\text{ELLIPTICITY} > 0.3$ and $\text{AREA} < 500$ pix (Mayya et. al 2008, Santiago-Cortez et., al 2010).

Simulations: a cluster is defined by a Gaussian intensity profile for a given FWHM and a total magnitude, with FWHM taking values of 2.0, 2.4, 3.0, 4.0, 5.0, 6.0, 7.0 and 8.0 pixels, and mags between 19 and 24.

Colour: for all SSC candidates we plot B-I colour. Is a bimodality distribution with a valley to $B-I = 1.5$



Colour-magnitude diagram

- GC candidates $B-I > 1.5$.
- SSPs with $Z=0.001$ (solid line) and 0.008 (dashed line).
- Vertical line GC with 12 Gyr, $Z=0.001$ at different masses.
- The reddening vectors (black arrows) with $A_v = 1$ mag.
- The chosen colour cut separates clusters older than 3 Gyr from the younger ones for unreddened SSPs.

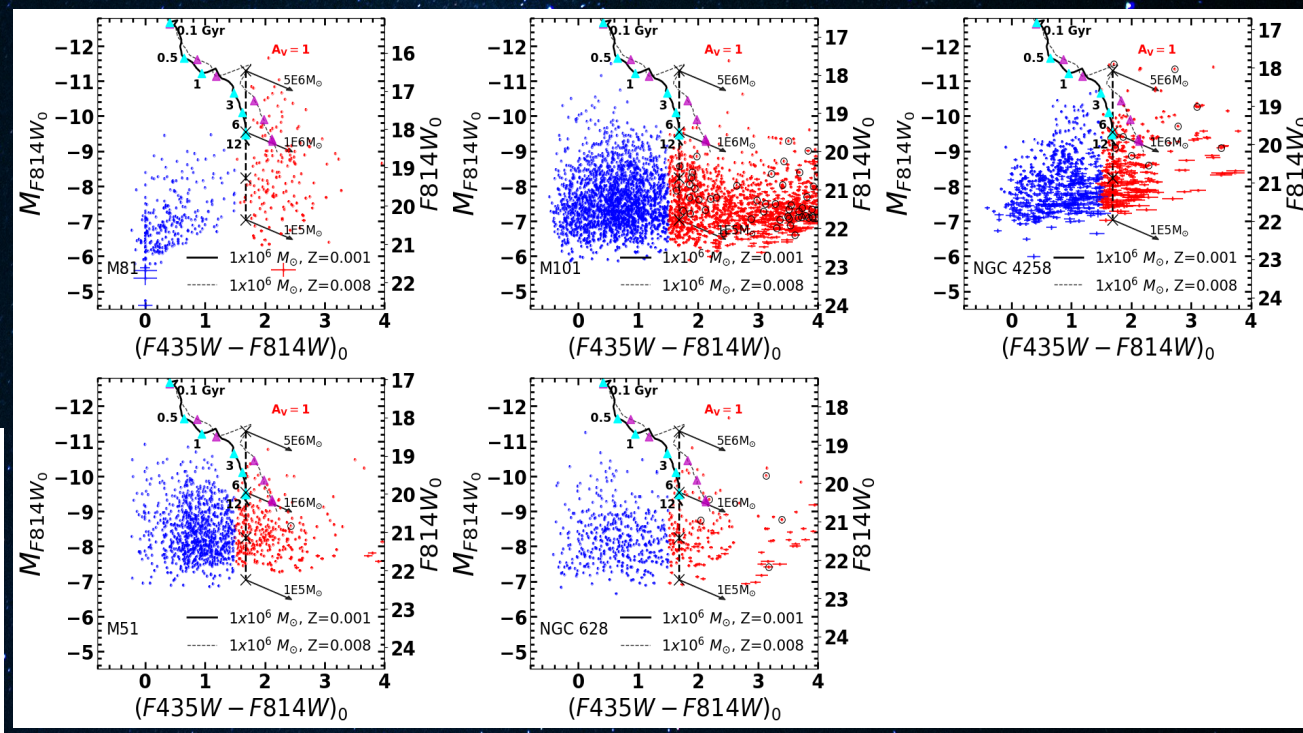
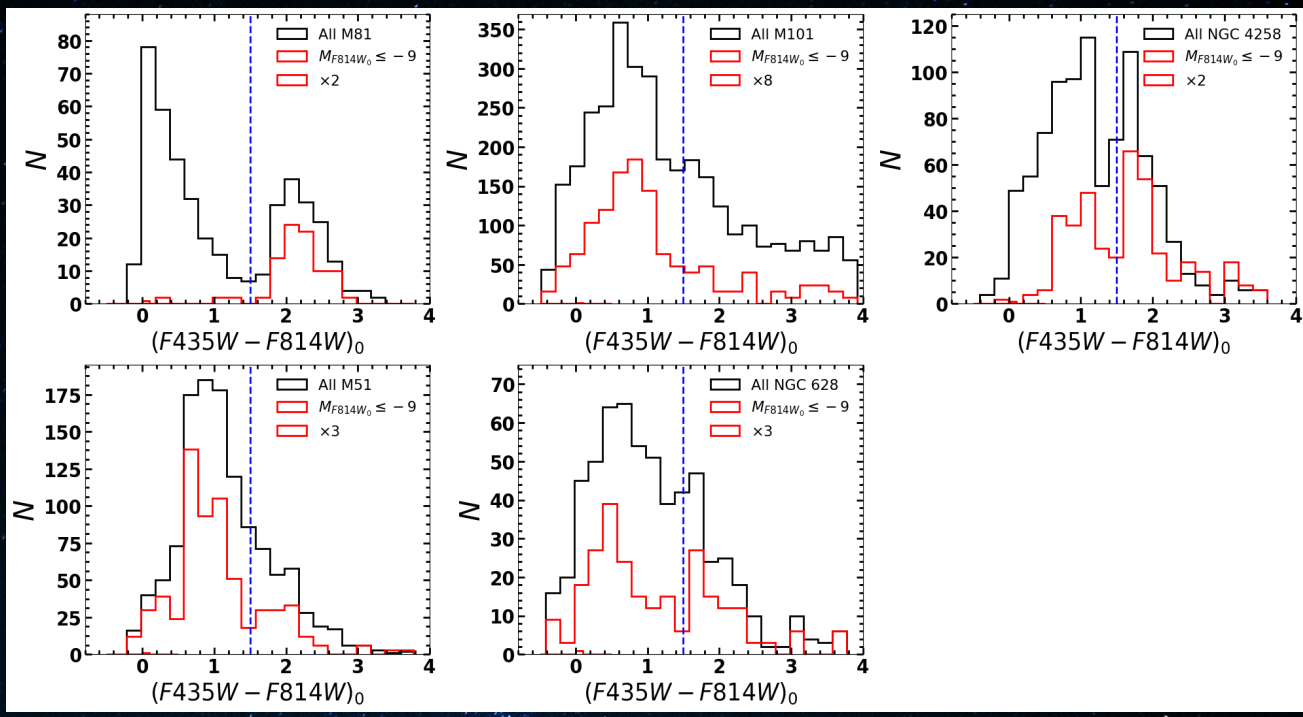


Table 3.- Source detection and stellar cluster selection.

Galaxy (1)	All N_{SSC+GC} (2)	NGC (3)	N_{GC}^U / N_{GC} (4)	N_{cont} / N_{GC} (5)	(6)
M81	565438	433	158	0.65	0.20
M101	1215533	3503	1202	0.15	0.31
NGC4258	1360607	936	334	0.38	0.33
M51	452747	1196	293	0.52	0.25
NGC628	224108	608	173	0.41	0.14

Colour-Colour Diagram:

- GC candidates with U-band (u , F336W) measure ($B-I > 1.5$).
- SSPs with different metallicities.
- The reddening vector (black arrow) with $A_V = 1$ mag.
- The reddened young SSCs that occupy the GC colours are contaminants, which are identified by red dots surrounded by circles of cyan colour.

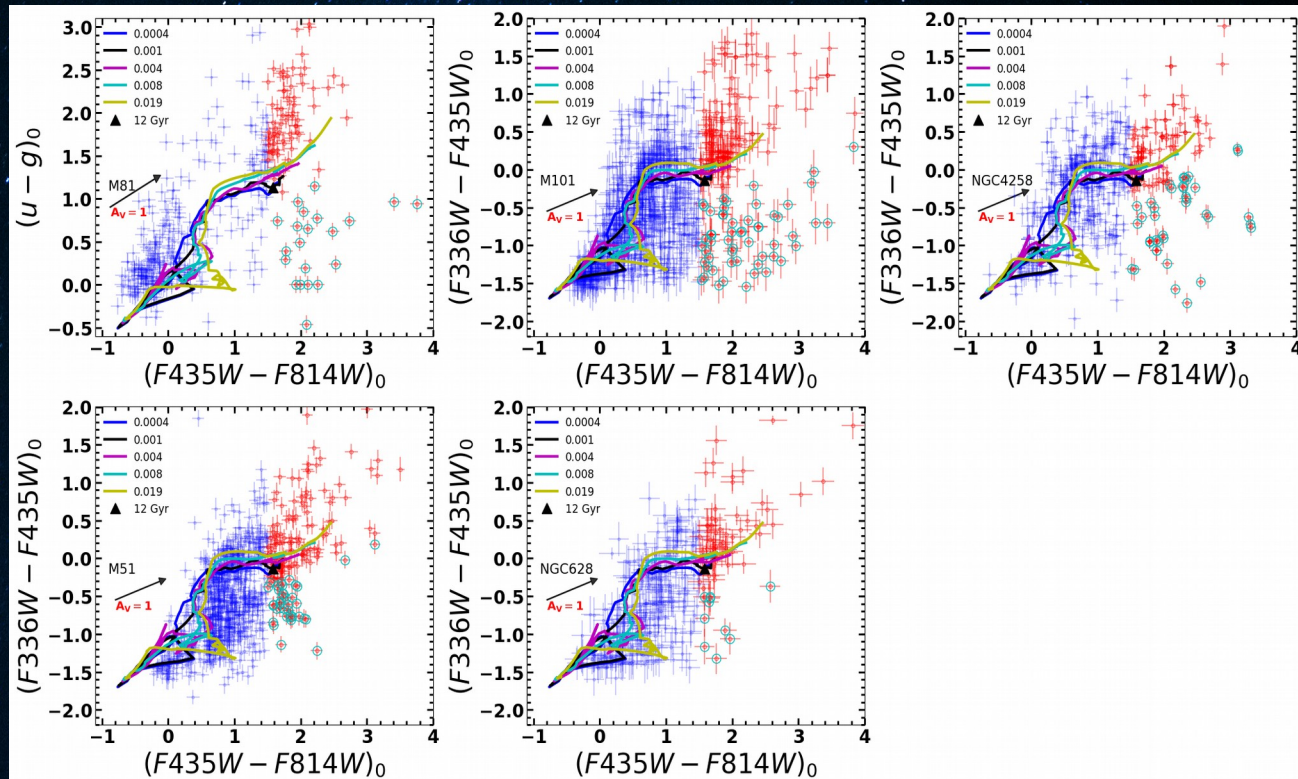
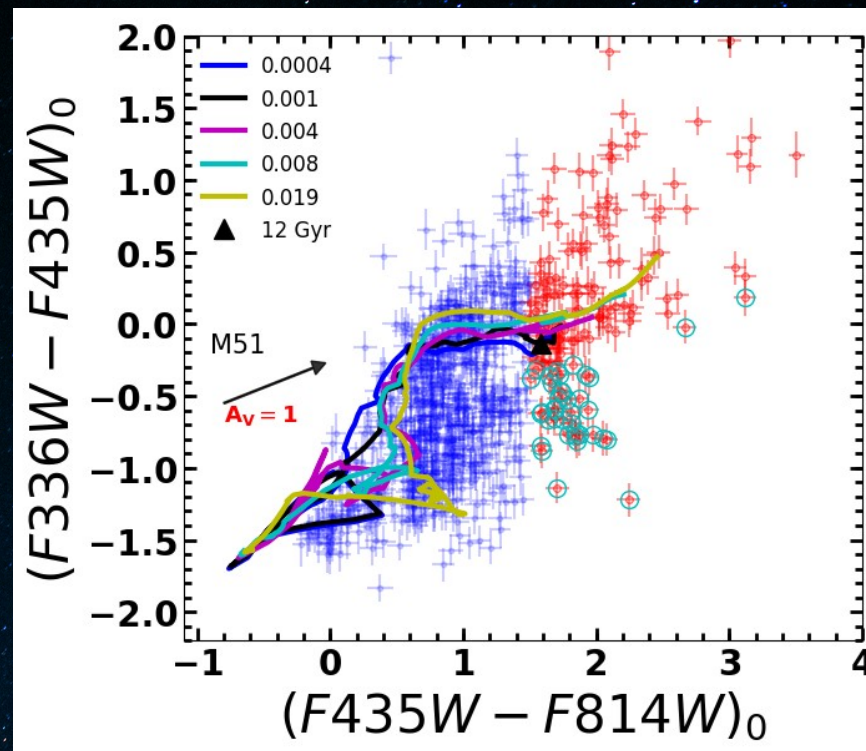


Table 3.- Source detection and stellar cluster selection.

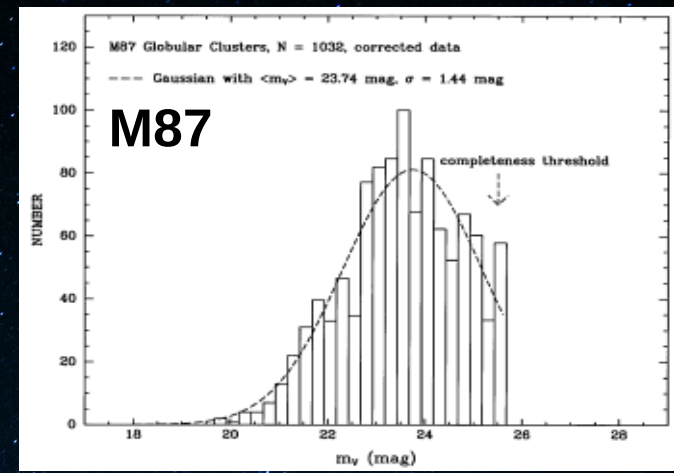
Galaxy (1)	All N_{SSC+GC} (2)	N_{GC} (3)	N_{GC}^U / N_{GC} (4)	N_{cont} / N_{GC} (5)	(6)
M81	565438	433	158	0.65	0.20
M101	1215533	3503	1202	0.15	0.31
NGC4258	1360607	936	334	0.38	0.33
M51	452747	1196	293	0.52	0.25
NGC628	224108	608	173	0.41	0.14

Luminosity Functions of Globular Clusters in five nearby spiral galaxies

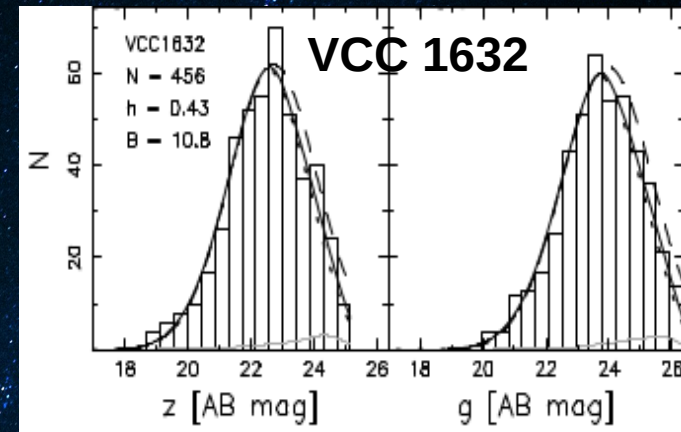
Globular Clusters Luminosity Function (GCLFs):

$$dN/dM = N_0 e^{-(M-M_0)^2/2\sigma^2}$$

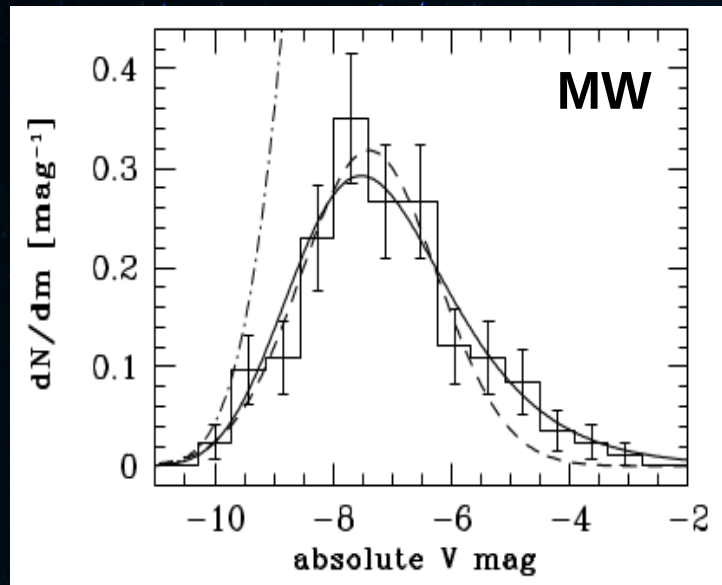
where $-7.3 < M_V < -7.5$ and $\sigma=1.1$, for Milky Way (eg., Harris 1996, Jordan et al. 2006)



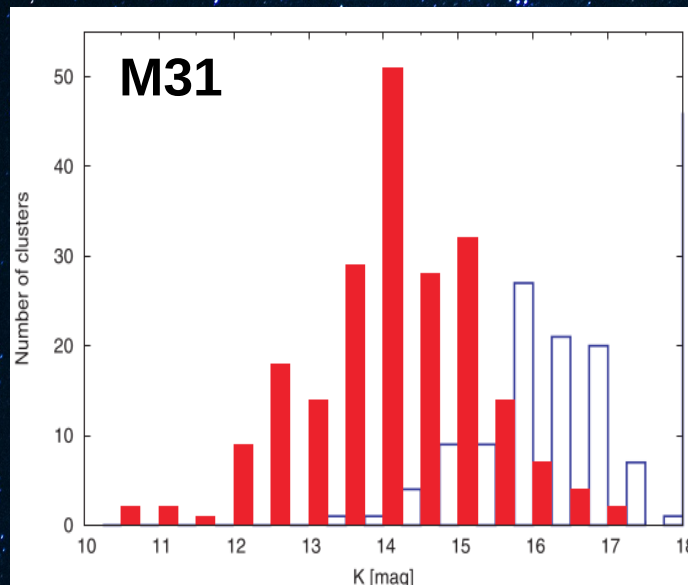
Whitmore et al. (1995)



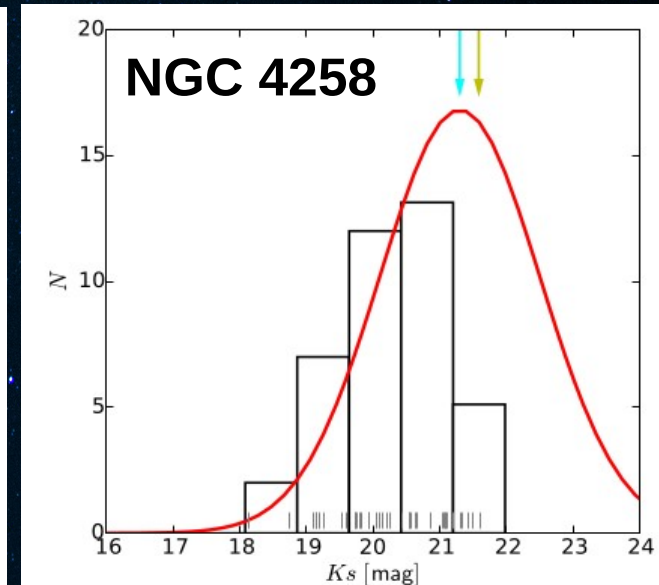
Jordan et al. (2006)



Jordan et al. (2006)



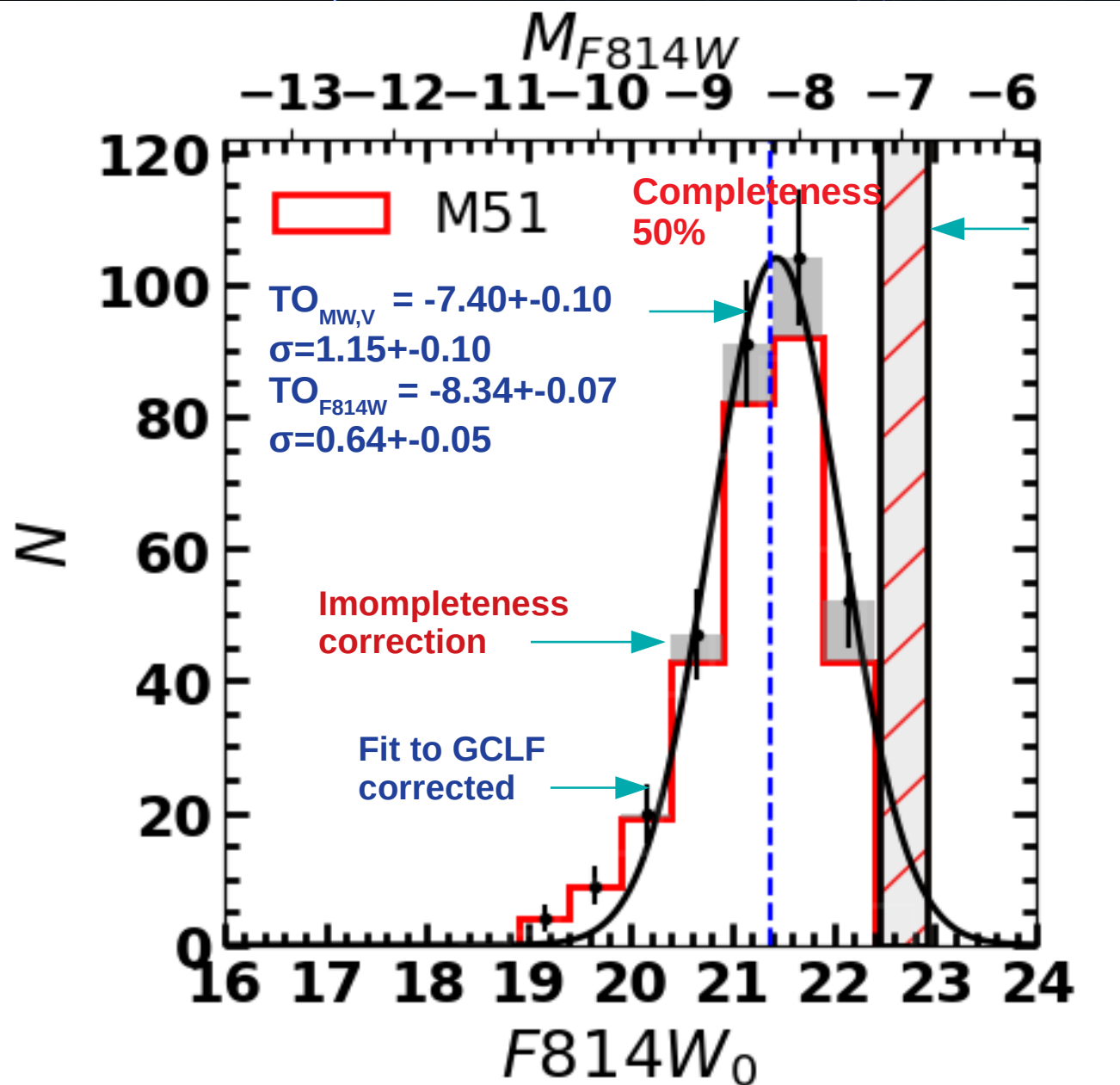
Peacock et al. (2010)



González-Lópezlira et al. (2017)

- **Some authors have suggested that GCLFs in elliptical galaxies is Universal (e.g. Hanes 1977b; Richtler 2003; Brodie & Strader 2006; Harris et al. 2014).**
- **What does it mean Universal?**
 - All have the same form**
 - All have the same peak or Turnover (TO)**
 - The same processes of formation and evolution (?)**
- **However, for spiral galaxies is not yet well defined.**
 - GCs detection is more difficult compared to elliptical galaxies:**
 - Spiral galaxies show substructure of the same scale size of GCs (spurious detections).**
 - Most of studies of GCs in spiral galaxies, are in edge-on galaxies.**
- **To build a complete GCLF is necessary:**
 - Spatial coverage.**
 - Spatial resolution.**
- **Are GCLFs the same for all spiral galaxies?**

M51 GCLF:



Fitting parameters:

$$TO_{\text{fit}} = 21.44 \pm 0.20,$$

$$\sigma = 0.64 \pm 0.05$$

$$m-M = 29.67 \pm 0.02$$

(Rodriguez et al. 2014)

$$TO_{\text{fit}} = -8.34 \pm 0.07$$

$$TO_V = -7.44 \pm 0.12$$

Diferencia vs MW:

$$\text{dif}_{TO} = -0.04,$$

$$\text{dif}_{\sigma} = -0.51$$

GCLFs:

For construct the GCLF:

- Aperture photometry
- Star cluster Simulations
- Structural parameters selection
- SExtractor
- Colour selection (B-I) and (U-B)
- Completeness corrections
- Star cluster Simulations
- Contaminants corrections
- (U-B)

The mean TO in four galaxies is:

$$\text{TO} = -7.38 \pm 0.13, \quad \sigma = 0.80 \pm 0.12,$$

while for MW:

$$\text{TO} = -7.40 \pm 0.10, \quad \sigma = 1.15 \pm 0.1$$

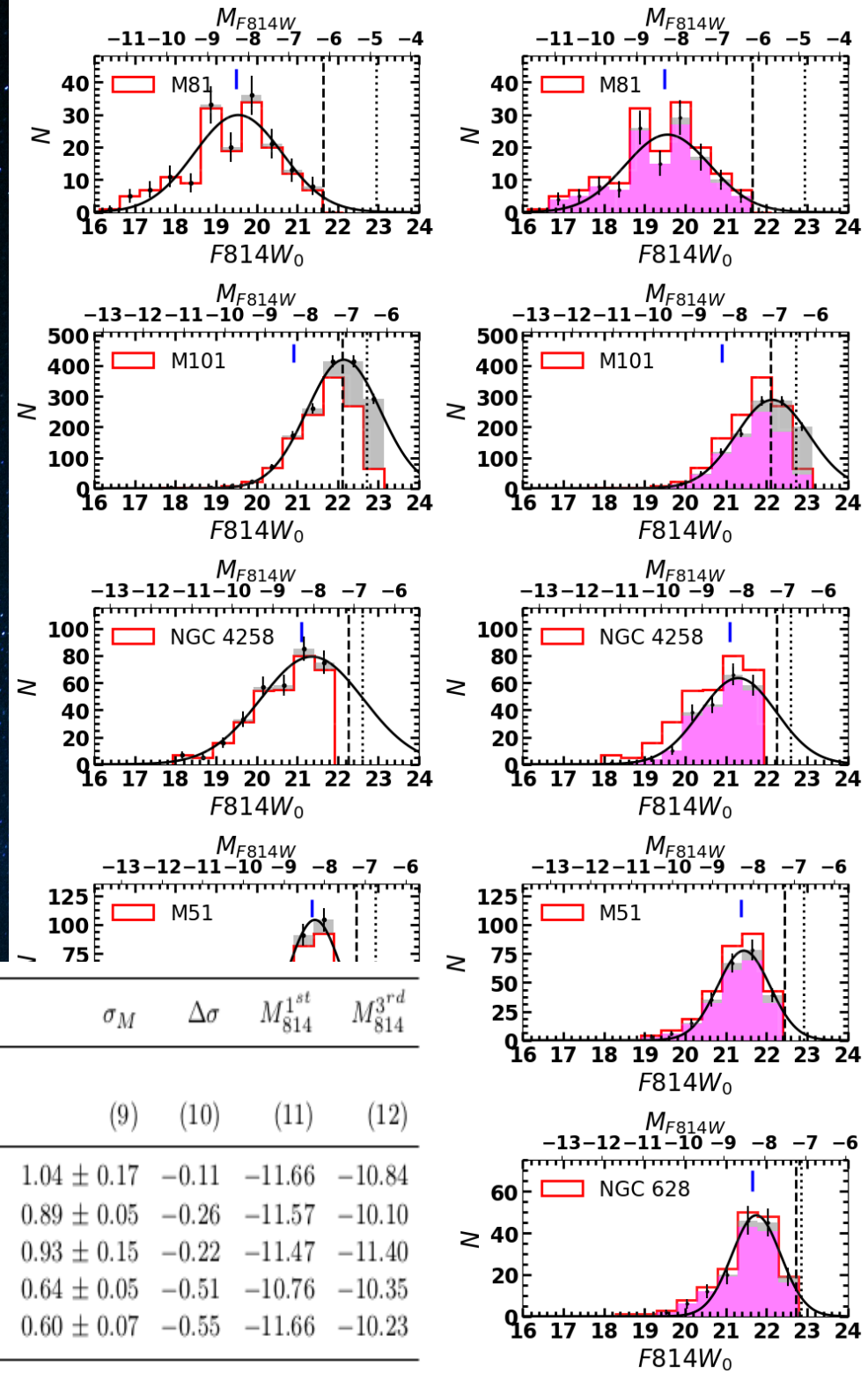
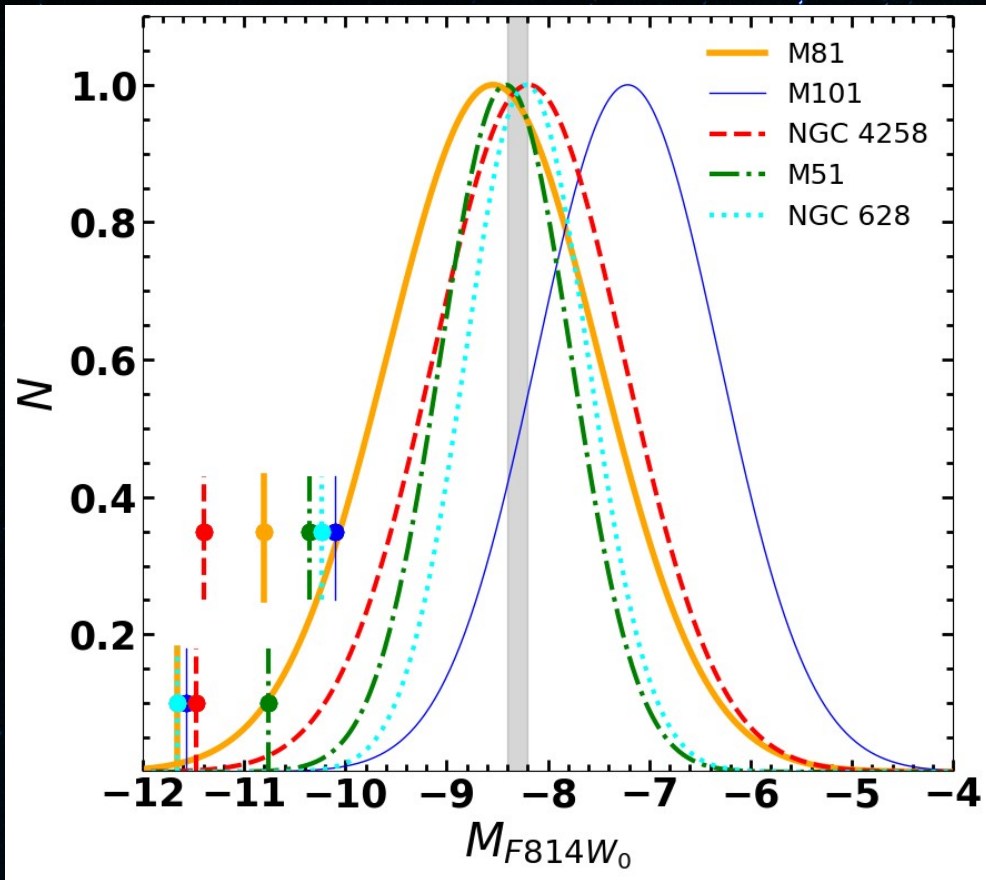


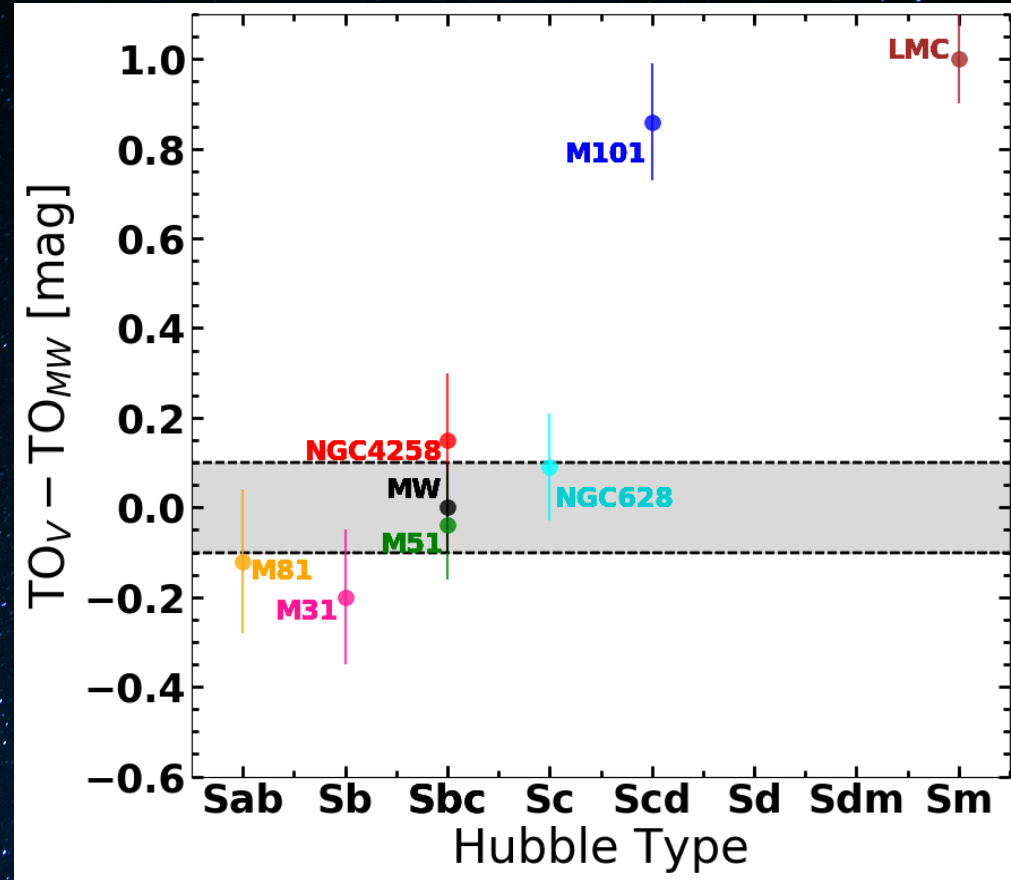
Table 4.- GCLF, fitting parameters.

Galaxy	N_{GC}			TO		ΔTO	σ_M	$\Delta\sigma$	M_{814}^{1st}	M_{814}^{3rd}	
(1)	Obs	fLF	total	$F814W_0$	M_{F814W_0}	M_{V_0}	(8)	(9)	(10)	(11)	(12)
M81	126	128 ± 13	235 ± 16	19.56 ± 0.12	-8.42 ± 0.13	-7.52 ± 0.16	-0.12	1.04 ± 0.17	-0.11	-11.66	-10.84
M101	1135	1644 ± 78	1401 ± 87	21.86 ± 0.05	-7.44 ± 0.08	-6.54 ± 0.13	0.86	0.89 ± 0.05	-0.26	-11.57	-10.10
NGC4258	222	303 ± 40	347 ± 41	21.30 ± 0.11	-8.15 ± 0.11	-7.25 ± 0.15	0.15	0.93 ± 0.15	-0.22	-11.47	-11.40
M51	243	261 ± 24	293 ± 27	21.44 ± 0.07	-8.34 ± 0.07	-7.44 ± 0.12	-0.04	0.64 ± 0.05	-0.51	-10.76	-10.35
NGC628	150	151 ± 16	157 ± 16	21.75 ± 0.05	-8.21 ± 0.06	-7.31 ± 0.12	0.09	0.60 ± 0.07	-0.55	-11.66	-10.23

GCLFs:



Normalized absolute F814W magnitude distribution of our sample of galaxies. The gray band indicate the TO magnitude of the MW GC. The band-width correspond to the TO uncertainty.



$TO_V - TO_{MW}$ vs the Hubble Type of host galaxies. The plot includes 5 galaxies from our sample and the MW, M31 and LMC galaxies. The error in the MW TO is indicated by the width of the gray band.

Some conclusions:

- We find that the LF of GCs in all the five analyzed galaxies is log-normal in nature, with the turn-over (TO) happening on the brighter side of the 50% incompleteness limiting.
- The mean of the $M_V(\text{TO})$ in 4 of our galaxies is -7.38 ± 0.13 , which is in excellent agreement with the values determined for GC population in the Milky Way $M_V(\text{TO}) = -7.40 \pm 0.10$ mag (Jordan et al. 2006).
- In the fifth galaxy M101, $M_V(\text{TO})$ is 0.86 mag fainter than the MW. We propose that this difference in $M_V(\text{TO})$ arises due to morphological differences, with spiral galaxies of the Hubble types Sc or earlier having a universal $M_V(\text{TO})$, whereas the Hubble types later than Sc have fainter $M_V(\text{TO})$.
- The universality of $M_V(\text{TO})$ in early-type spirals is due to the classical GCs dominating the GC population, whereas in late-type spirals GC population is often dominated by old disk clusters, which are in general less massive, and hence fainter than the classical GCs, but otherwise share the same observational properties as the classical GCs.

Second part: Spectroscopic results

Generalities:

- What do we want to do with the spectra?

Date the star clusters

- How will we do it?

In three steps: 1.- Metallicity (Spectral indices)
2.- Extinction (SSP)
3.- Age (SSP)

- Spectral dating is age-colour degeneration free.
- We use simple stellar populations (SSP) spectra with ages ranging from 1 to 13.5 Gyr, and metallicities: $Z=0.0001$, 0.0004 , 0.004 , 0.008 , 0.02 , y 0.05 .
- For this purpose, the IspecFit (INAOE Spectra Fitting) software was created.
- We have analyzed 42 GC candidates spectra in M81.

Spectroscopic campings:

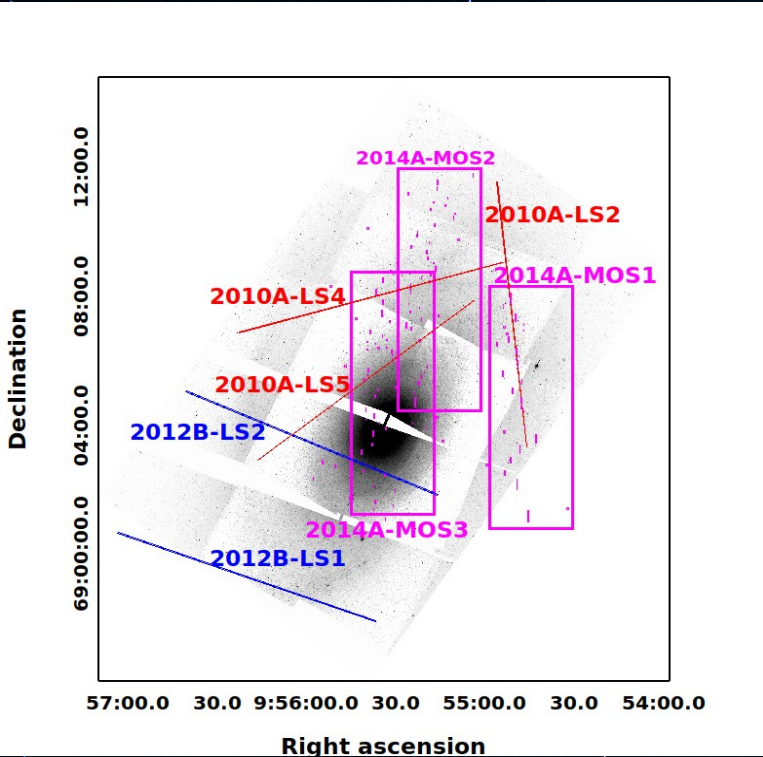
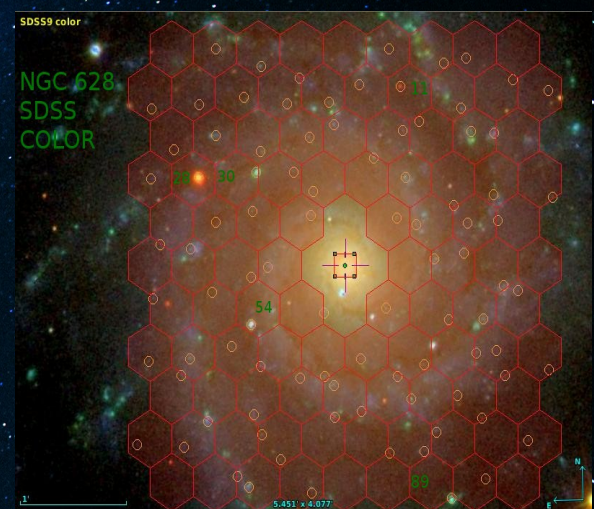
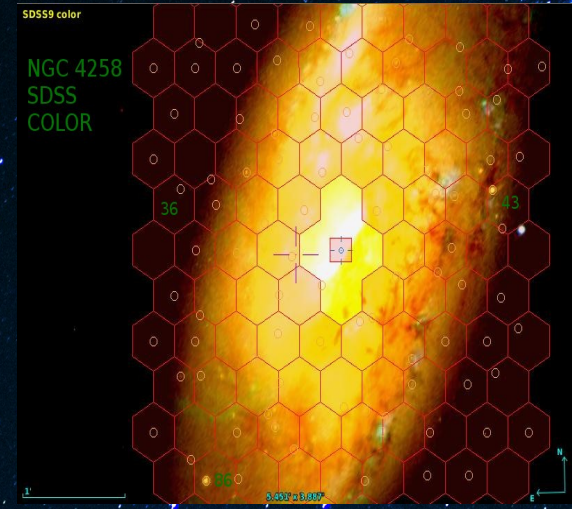
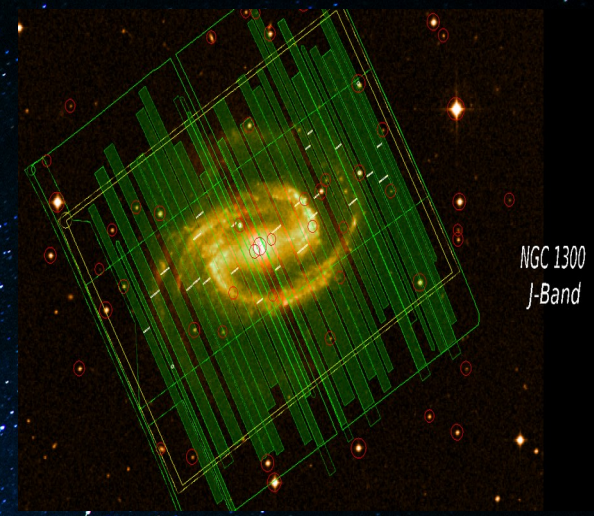
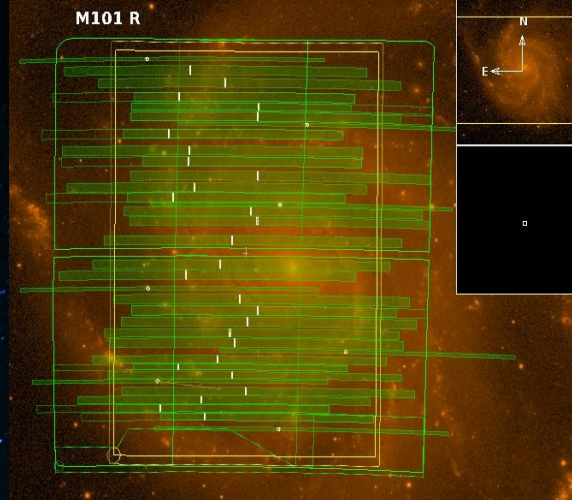
OSIRIS:

- 8 OBs en M81
- 3 OBs en M101
- 1 OB en NGC 1300*

MEGARA:

- NGC 4258*
- NGC 628*

*Not observed yet



Run/Mode (1)	PI (2)	Date (3)	PA (4)	SW (5)	Exp. time (6)	AM (7)	Seeing (8)	Night (9)	Std (10)	N_{GC} (11)
gtc10aob002 2010A-LS2	D. Rosa-González	2010-04-05	6.24	1.00	3×900	1.33	0.80	G	Feige34	3
gtc10aob004 2010A-LS4	D. Rosa-González	2010-04-05	105.20	1.00	3×900	1.56	0.80	G	Feige34	1
gtc10aob005 2010A-LS5	D. Rosa-González	2010-04-06	127.20	1.00	3×900	1.43	0.80	F	Feige34	1
gtc12bob001 2012B-LS1	Y. D. Mayya	2013-01-12	250.50	1.23	3×1500	1.31	0.79	D	Feige34	2
gtc12bob002 2012B-LS2	Y. D. Mayya	2013-01-12	247.00	1.23	3×1500	1.40	0.97	D	Feige34	2
gtc14aob001 2014A-MOS1	Y. D. Mayya	2014-04-03	0.00	1.20	3×1308	1.31	0.90	D	Ross 640	5
gtc14aob002 2014A-MOS2	Y. D. Mayya	2014-03-23	0.00	1.20	3×1308	1.35	1.00	D	Ross 640	8
gtc14aob003 2014A-MOS3	Y. D. Mayya	2014-04-03	0.00	1.20	3×1308	1.34	0.80	D	Ross 640	25

Notes: (1) Observation run. (2) Principal investigator (PI). (3) observational date (year-month-date). (4) Position angle ($^{\circ}$) of the slit as measured on the astrometrized image. (5) Slit-width (arcsec). (6) Exposure time (number of exposures \times integration time in seconds). (7) Mean airmass of the three integrations. (8) Seeing ($''$). (9) Night (G=grey or D=dark), clear skies (cirrus reported only for 2010A-LS5). (10) Standard star name (11) Number of GCs in each observation.

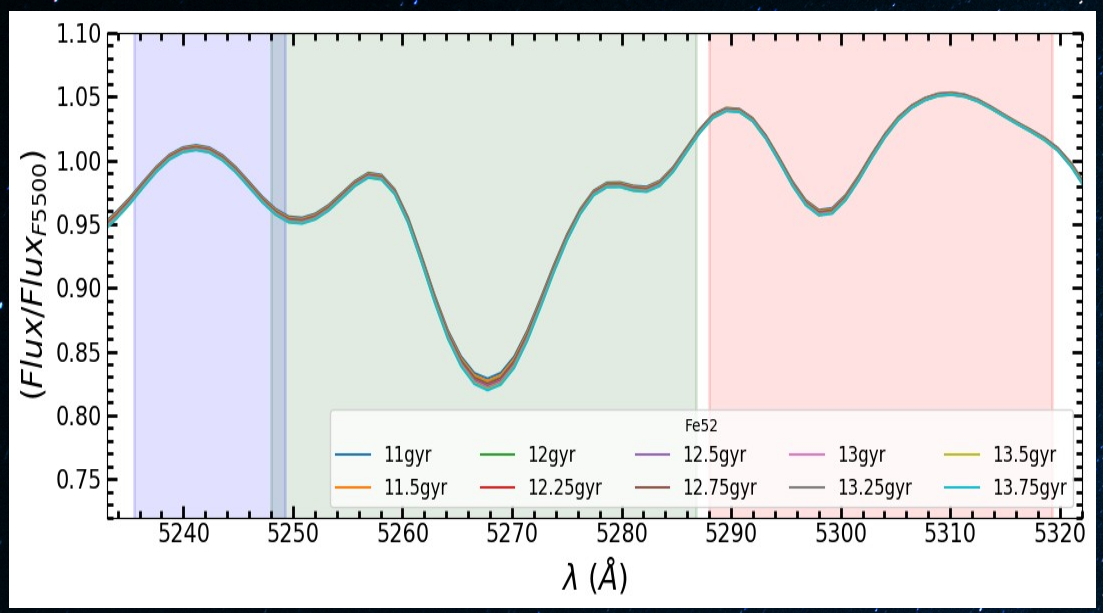
Spectral fittings software:

- **STARLIGHT**: is a software, based on Fortran 77, programmed to fit a composed spectrum model $M(\lambda)$ to an observed spectrum $O(\lambda)$, that is the sum of N^* spectral components
- **ULySS** (University of Lyon Spectroscopic analysis Software): fit a spectra with a lineal combination of non-linear combined convolutions with a distribution of velocities in the line of sight and is polynomial multiplicative.
- **SINOPSIS** (SimulatiNg Optical Spectra with Stellar populations models): is a code created to reproduce the main characteristics of observed spectra of galaxies (at rest) in a range from UV to near infrared.
- **IspecFit** (INAOE Spectra Fitting, tentative name): is a software specialized in the analysis of old stellar populations. It is based on IDL and Python languages. It performs the spectral fit in three steps: 1) metallicity estimation using spectral indices, 2) extinction estimation and 3) age estimation using SSPs.

Spectral indices:

$$I = -2.5 \log_{10} \left[2 \int_{\lambda_1}^{\lambda_2} \frac{F_I}{F_{BC} + F_{RC}} d\lambda \right]$$

where F_I is the flux in the index width
 F_{BC} y F_{RC} are the pseudo-continuum
 fluxes enclosing the index range.



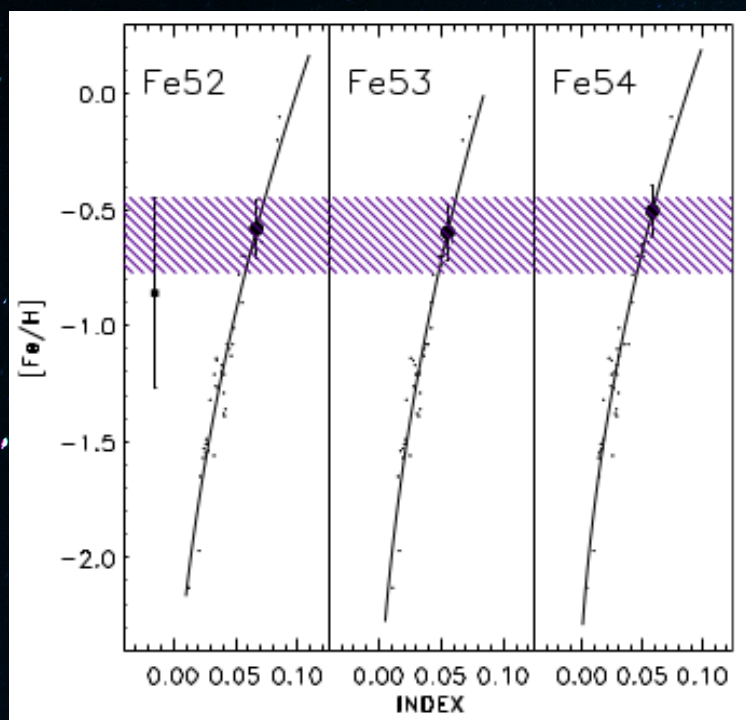
Element	Blue Continuum		Index		Red Continuum	
D	3800.00	4000.00	4000.00	4200.00	0000.00	0000.00
CNR	4082.00	4118.50	4144.00	4177.50	4246.00	4284.75
G	4268.25	4283.25	4283.25	4317.00	4320.75	4335.75
MgH	4897.00	4958.00	5071.00	5134.75	5303.00	6366.75
Mg2	4897.00	4958.00	5156.00	5197.25	5303.00	6366.75
Mgb	5144.50	5162.00	5162.00	5193.25	5193.25	5207.00
Fe52	5235.50	5249.25	5248.00	5286.75	5288.00	5319.25
Fe53	5307.25	5317.25	5314.75	5353.50	5356.00	5364.75
Fe54	5376.25	5387.50	5387.50	5415.00	5415.00	5425.00

INDEX DEFINITIONS						
Name	Index Bandpass	Pseudocontinua	Units	Measures	Error ¹	Notes
01	CN ₁	4143.375-4178.375	4081.375-4118.875 4245.375-4285.375	mag	CN, Fe I	0.021
02	CN ₂	4143.375-4178.375	4085.125-4097.625 4245.375-4285.375	mag	CN, Fe I	0.023 2
03	Ca4227	4223.500-4236.000	4212.250-4221.000 4242.250-4252.250	Å	Ca I, Fe I, Fe II	0.27 2
04	G4300	4282.625-4317.625	4287.625-4283.875 4320.125-4336.375	Å	CH, Fe I	0.39
05	Fe4383	4370.375-4421.625	4360.375-4371.625 4444.125-4456.625	Å	Fe I, Ti II	0.53 2
06	Ca4455	4453.375-4475.875	4447.125-4455.875 4478.375-4493.375	Å	Ca I, Fe I, Ni I, Ti II, Mn I, V I	0.25 2
07	Fe4531	4515.500-4560.500	4505.500-4515.500 4561.750-4580.500	Å	Fe I, Ti I, Fe II, Ti II	0.42 2
08	Fe4668	4635.250-4721.500	4612.750-4631.500 4744.000-4757.750	Å	Fe I, Ti I, Cr I, Mg I, Ni I, C ₂	0.64 2
09	Hβ	4847.875-4876.625	4827.875-4847.875 4876.625-4891.625	Å	Hβ, Fe I	0.22 3
10	Fe5015	4977.750-5054.000	4946.500-4977.750 5054.000-5065.250	Å	Fe I, Ni I, Ti I	0.46 2,3
11	Mg ₁	5069.125-5134.125	4895.125-4957.625 5301.125-5366.125	mag	MgH, Fe I, Ni I	0.007 3
12	Mg ₂	5154.125-5196.625	4895.125-4957.625 5301.125-5366.125	mag	MgH, Mg b, Fe I	0.008 3
13	Mg b	5160.125-5192.625	5142.625-5161.375 5191.375-5206.375	Å	Mg b	0.23 3
14	Fe5270	5245.650-5285.650	5233.150-5248.150 5285.650-5318.150	Å	Fe I, Ca I	0.28 3
15	Fe5335	5312.125-5352.125	5304.625-5315.875 5353.375-5363.375	Å	Fe I	0.26 3
16	Fe5406	5387.500-5415.000	5376.250-5387.500 5415.000-5425.000	Å	Fe I, Cr I	0.20 2,3
17	Fe5709	5698.375-5722.125	5674.625-5698.375 5724.625-5738.375	Å	Fe I, Ni I, Mg I Cr I, V I	0.18 2
18	Fe5782	5778.375-5798.375	5767.125-5777.125 5799.625-5813.375	Å	Fe I, Cr I Cu I, Mg I	0.20 2
19	Na D	5878.625-5911.125	5862.375-5877.375 5923.875-5949.875	Å	Na I	0.24
20	TiO ₁	5938.375-5995.875	5818.375-5850.875 6040.375-6105.375	mag	TiO	0.007
21	TiO ₂	6191.375-6273.875	6068.375-6143.375 6374.375-6416.875	mag	TiO	0.006

-Top: Lick indices (Worthey et al. 1994).
 -Left: Lick indices to age and metallicity
 estimation (Mayya et al. 2013;
 Rodríguez-Merino in preparation)

Metallicity estimation:

For metallicity estimation we used the method described in Maya et al. (2013). It uses tree iron spectral indices: Fe52, Fe53 and Fe54. It was calibrated using 41 MW-GCs from Schiavon et al. (2005).

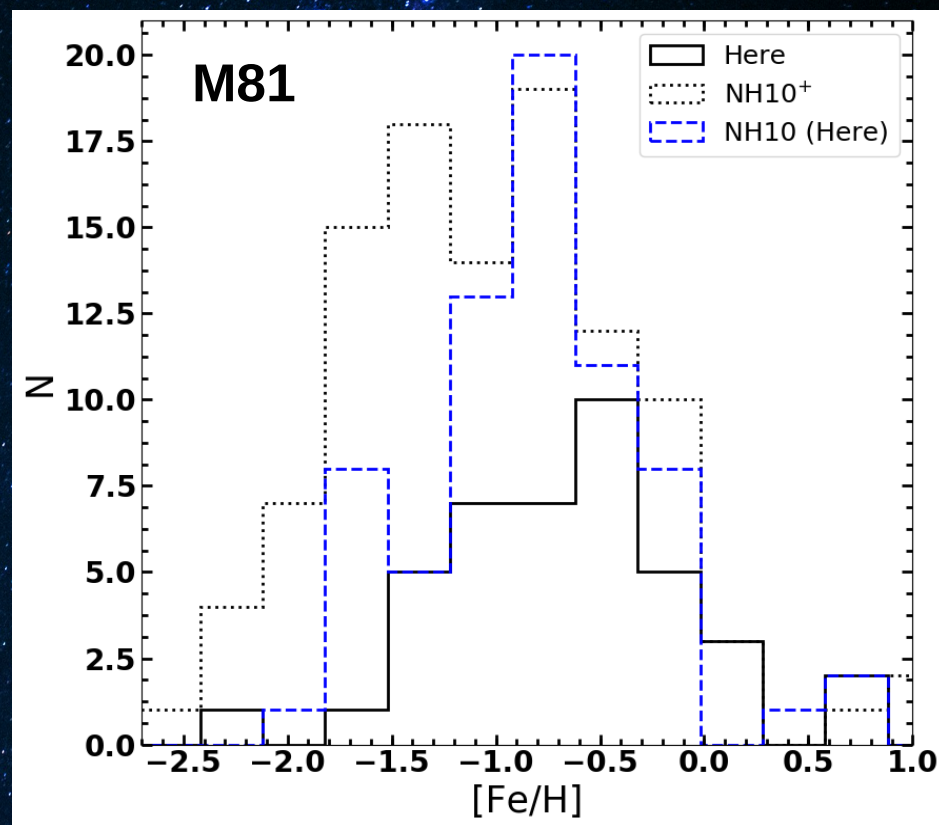


Maya et al. (2013)

8 de junio 2021

$$[Fe/H] - k^2 = 4p(\text{Index} - h)$$

where k , p and h are the polynomial coefficients.



$$\mu_{[Fe/H]} = -1.06 \pm 0.08 \quad (\text{Nantais et al., 2010})$$

$$\mu_{[Fe/H]} = -0.63 \pm 0.10 \quad (\text{This work})$$

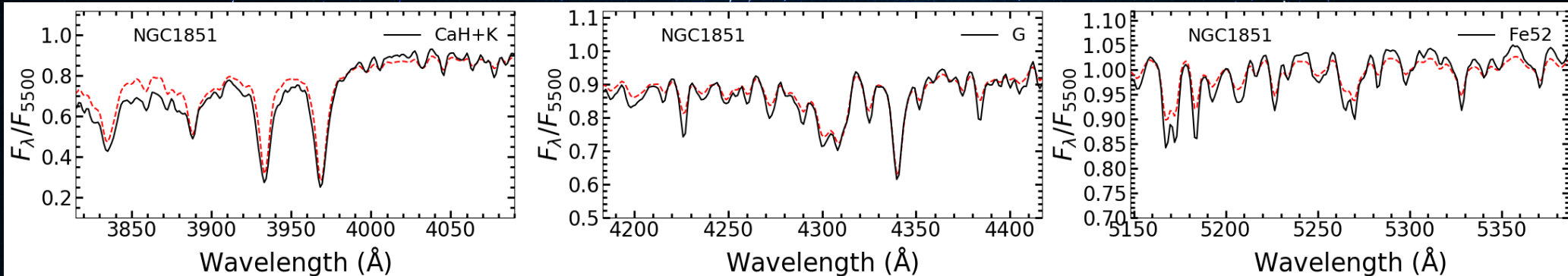
Fit spectral method:

- Index estimation (Brodie & Huchra 1990).
- Metallicity estimation with spectral indexes: Fe52, Fe53 y Fe54 (Mayya 2013, Lino-Merino in prep.).
- Extinction estimation (Cardelli et al. (1989).
- Age using with a χ^2 statistic:

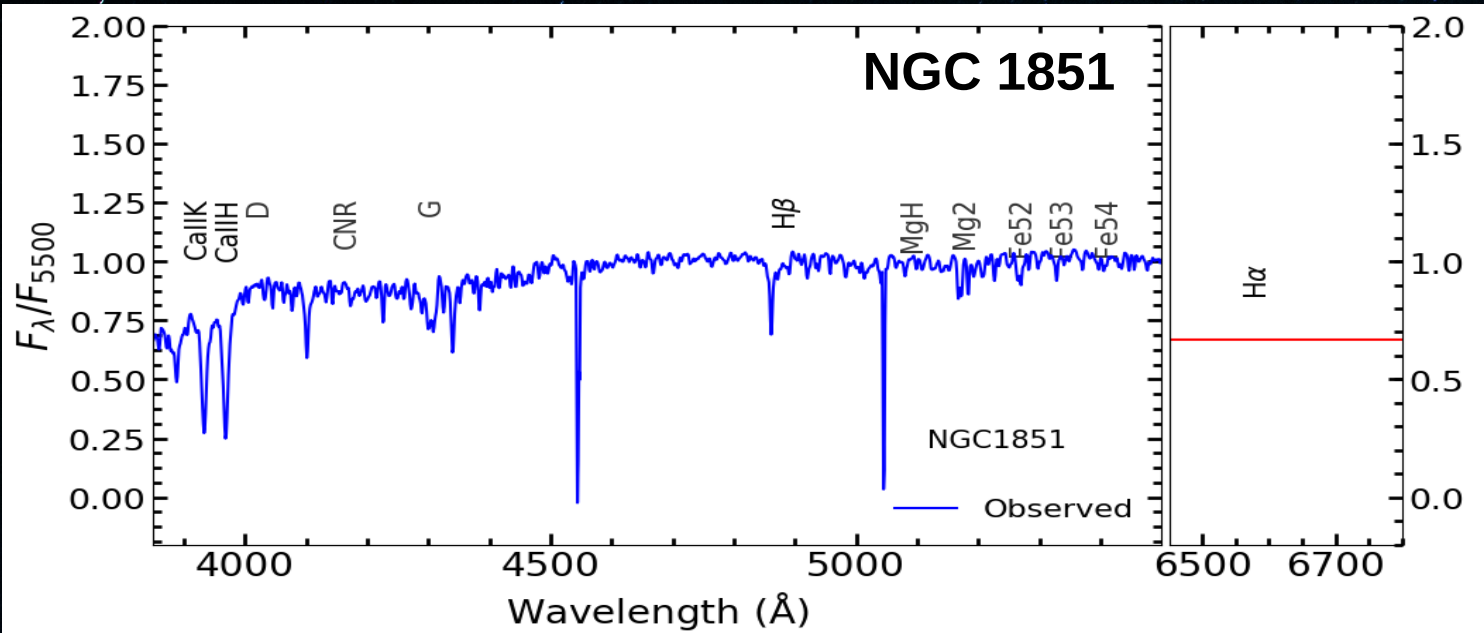
$$\chi^2 = \frac{1}{N} \sum_{i=1}^n \left(\frac{I_{obs,i} - I_{mod,i}}{\sigma_{obs,i}} W \right)^2$$

where N is the number of indexes, $I_{obs,i}$ and $I_{mod,i}$ are the observed and model index respectively. W is the statistical weight of the i -th index and sigma is the index error (Mayya et al. 2004).

- SSP ages range from 1 to 13.75 Gyr (Bruzaul & Charlot 2003).
- Initial function mass : Kroupa, Salpeter y Chabrier.
- Metallicities: $Z=0.0001, 0.0004, 0.004, 0.008, 0.02, y 0.05$.

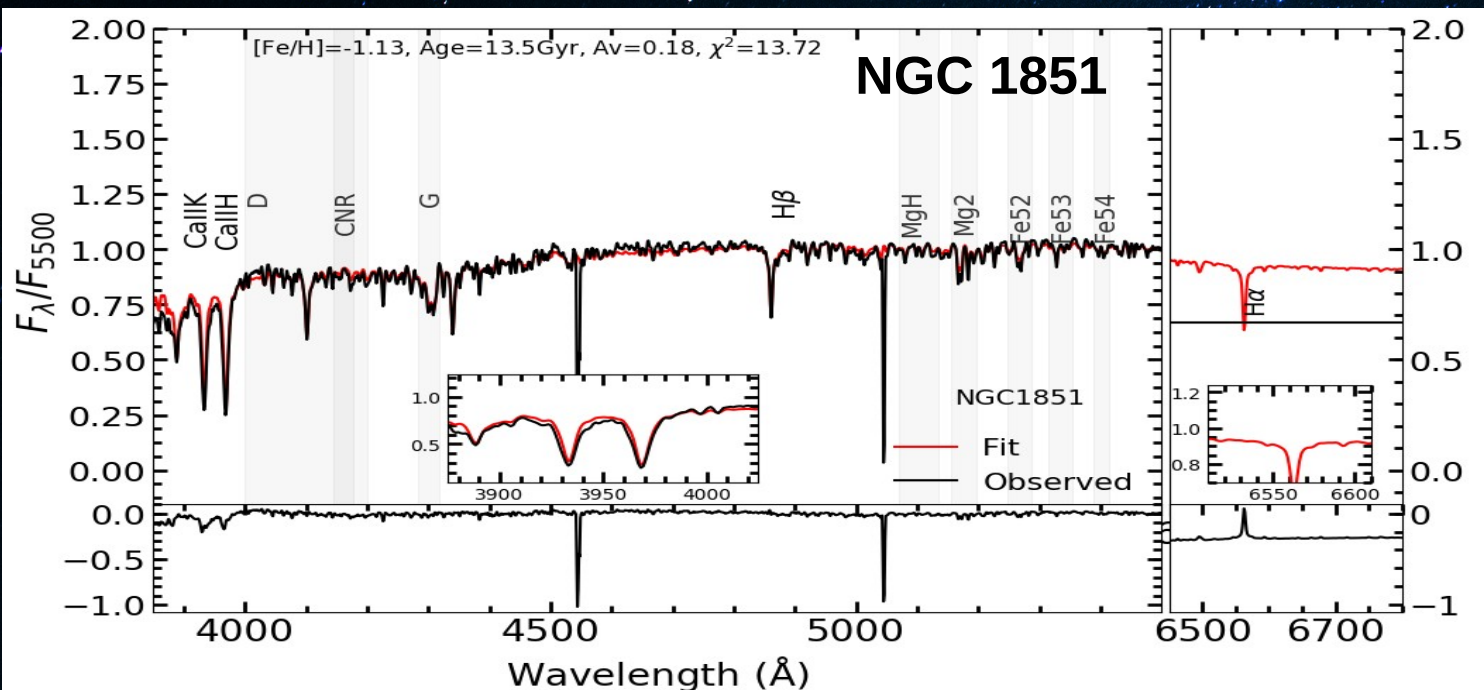


Spectral fit proof in MW-GC:



From Schiavon et al., (2005):

- 41 MW-GC spectra. Observed with Telescopio Blanco de 4m.
- $\Lambda = 3350\text{--}6430 \text{ \AA}$,
- Resolution 3.1 \AA in FWHM



NGC 1851:

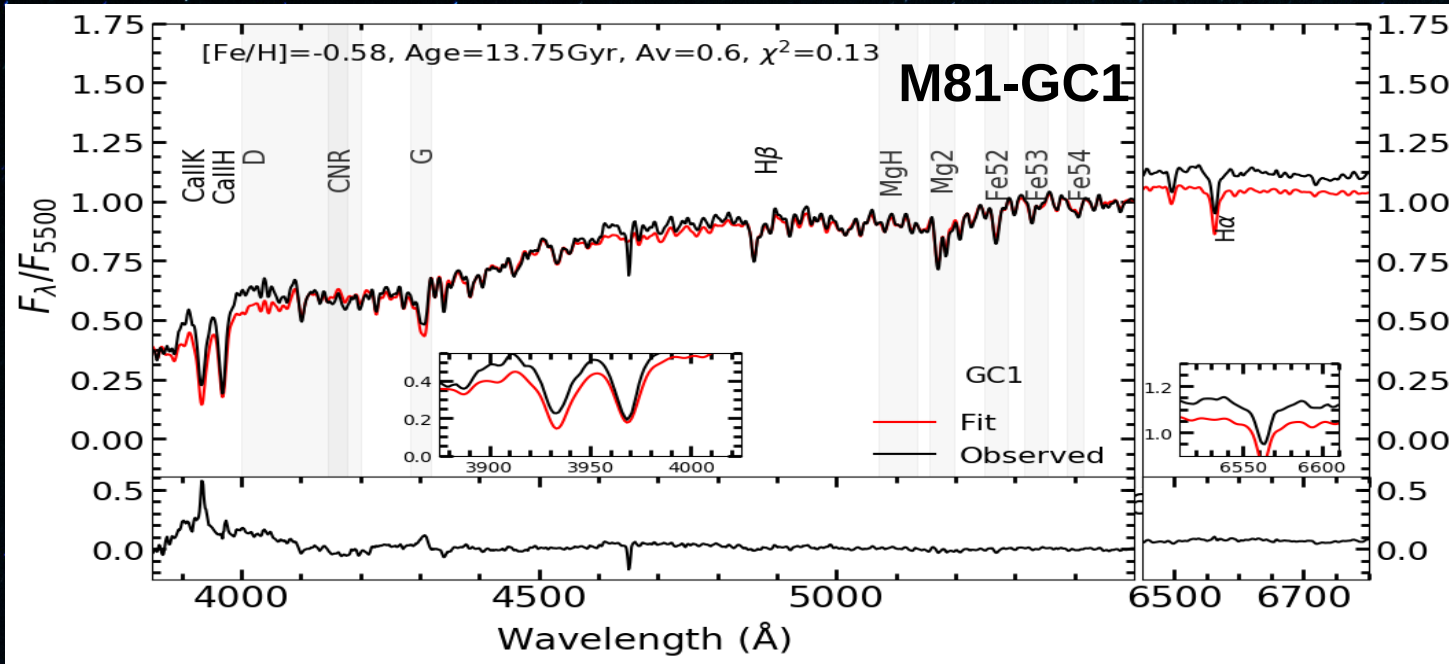
$[\text{Fe}/\text{H}] = -1.13$
 Age = 13.5 Gyr
 $A_v = 0.18$

Comparison:

$[\text{Fe}/\text{H}] = -1.18$
 De Angeli et al. (2005)

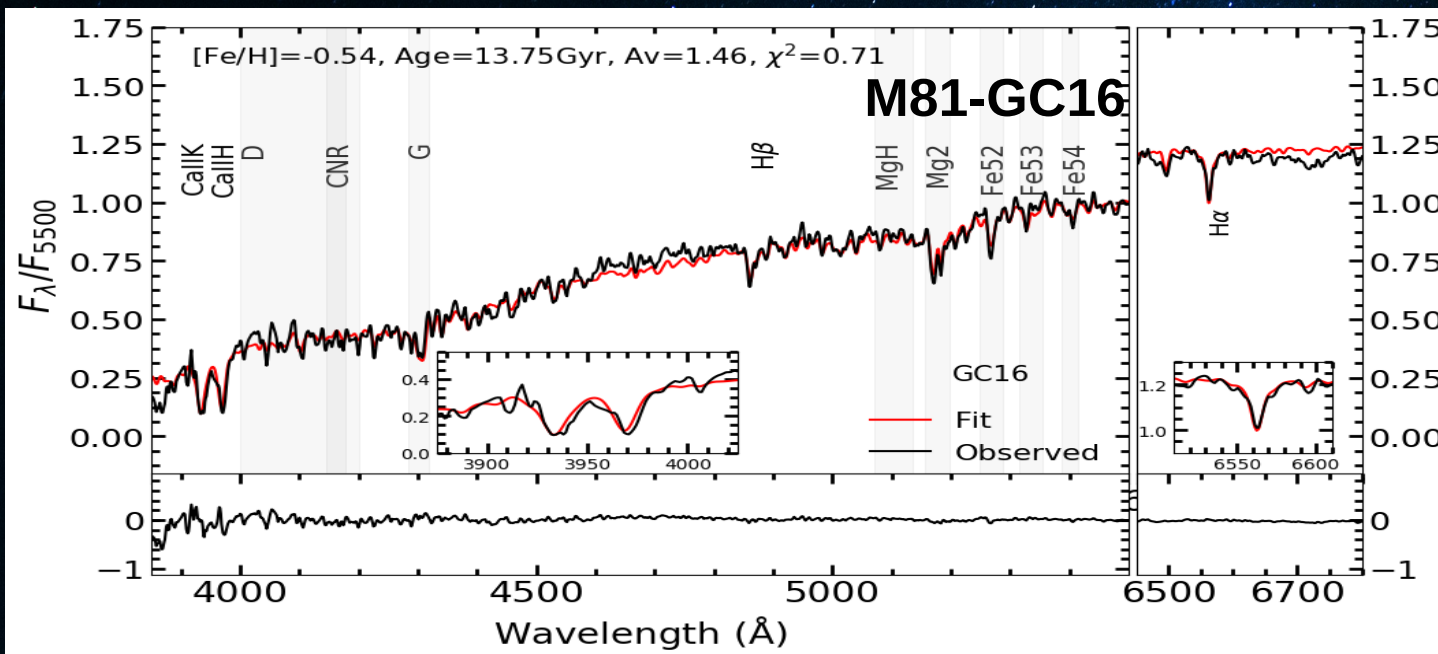
Age = 10.6 ± 2.1 Gyr
 Momany et al. (2003)

M81 GC candidates:



M81-GC1:
[Fe/H] = -0.58
Age = 13.75 Gyr
 $A_v = 0.6$

Comparison:
[Fe/H] = -0.60
Edad > 13 Gyr
(Mayya et al. 2013)



M81-GC16
[Fe/H] = -0.54
Age = 13.75 Gyr
 $A_v = 1.46$

Some conclusions of spectroscopic part:

- Our results show a GCs mean metallicities higher than the reported in Natais et al. (2010).
- We develop a specialized software to fit old stellar populations spectra (IspecFit).
- IspecFit can be applied to estimate: 1) metallicity, 2) extinction and 3) age of stellar population.
- We have analyzed 42 GC candidates in M81 galaxy. We confirm that ~30 objects of our sample are GC. The remaining 12 candidate could not be verified to be GC due to their low S/N ratio.

General Conclusions:

- We developed (improved) a photometric method for detected SSC in spiral galaxies.
- We can establish the presence of SSC in our sample of galaxies.
- In the GC system in four of five galaxies here studied we found a TO similar to MW.
- We developed a specialized software to fit old stellar populations spectra.
- We still dating the blue and red SSC populations. For this we will use a photometric method.
- When we will date the blue and red part we can recover the star formation history.
- We are awaiting new spectroscopic observations from MEGARA.

Luminosity functions of globular clusters in five nearby spiral galaxies using HST/ACS images

Luis Lomelí-Núñez[★], Y.D. Mayya, L.H. Rodríguez-Merino, P.A. Ovando,
and D. Rosa-González

Instituto Nacional de Astrofísica Óptica y Electrónica, Luis Enrique Erro 1, Tonantzintla 72840, Puebla, Mexico

- The results presented in the previous slides have been submitted to MNRAS in the article titled: ‘Luminosity functions of globular clusters in five nearby spiral galaxies using HST/ACS images’
- We sent the answer in May 23th, 2020.
- We response in May 18th 2021.

GTC/OSIRIS spectroscopic age estimation of globular clusters in M81

Luis Lomelí-Núñez,^{1★} Y.D. Mayya,¹ L.H. Rodríguez-Merino,¹ P.A. Ovando,¹
Jairo A. Alzate,² B. Cuevas-Otahola,¹ Javier Zaragoza-Cardiel,¹ D. Rosa-González¹
Gustavo Bruzual² and V.M.A Gómez-González²

¹*Instituto Nacional de Astrofísica Óptica y Electrónica, Luis Enrique Erro 1, Tonantzintla 72840, Puebla, México*

²*Instituto de Radioastronomía y Astrofísica, UNAM, Campus Morelia, Michoacán, México, C.P. 58089, México*

GRACIAS